

Molybdenum and Chlorine X-Ray Emission  
from Alcator A

J.E. Rice, E.S. Marmor and T. Coan  
Plasma Fusion Center/Francis Bitter National Magnet  
Laboratory, M.I.T.

S. L. Allen

Johns Hopkins University

R.D. Cowan

Los Alamos Scientific Laboratory

PFC/RR-80-5

PFC/JA-80-1

Abstract

High resolution ( $\Delta\lambda/\lambda \approx .015$ ) x-ray spectra in the wavelength region  $3.7 + 6.2 \text{ \AA}$  ( $3.4 + 2.0 \text{ keV}$ ) have been collected from the Alcator tokamak using a flat crystal Bragg monochromator. Molybdenum L lines and chlorine K lines have been observed and charge state identifications have been made by comparison with calculations.

## I. Detection System

A flat crystal monochromator with a pentaerythritol (PET,  $2d = 8.742 \text{ \AA}$ ) crystal has been installed on the Alcator A tokamak. A proportional counter was used as the photon detector and overall time resolution of the detection system was about 100  $\mu\text{s}$ . Spectra have been obtained by scanning in wavelength on a shot to shot basis during a sequence of identical discharges. Wavelength calibration was achieved by using the L series of  $\text{Mo}^{\text{II}}$  produced by a Henke tube. Accuracy of wavelength determinations is about  $\pm .005 \text{ \AA}$ .

## II. Observations on Alcator A

Fig. 1 shows the time history of a typical Alcator A discharge at 60 kG. The top traces are the plasma current and average electron density (50 kA/div and  $1 \times 10^{14} \text{ cm}^{-3}$ /fringe). The third trace is the monochromator signal at  $4.76 \text{ \AA}$  (2.60 keV) and the bottom trace is the total soft x-ray flux above 1.5 keV from a surface barrier diode (SBD) viewing along a chord through the center of the plasma. The time scale is 20 ms/div. During the steady state portion of this discharge, when the average electron density was  $2.9 \times 10^{14} \text{ cm}^{-3}$ , the plasma current was 160 kA, and the sawtooth oscillations were well developed (between 70 and 110 ms), the central electron temperature was  $\sim 900 \text{ eV}$ . At the startup phase of the discharge, around 20 ms when the

density was  $5 \times 10^{13} \text{ cm}^{-3}$ , the electron distribution was non-thermal but (in the energy region of interest) can be characterized by a hot Maxwellian with  $T_e \sim 1800 \text{ eV}$ . Note the large spike on the SBD and spectrometer signals at this time.

Fig. 2 is the spectrum at 100 ms for a series of discharges similar to the one shown in Fig. 1, obtained by scanning in wavelength on a shot to shot basis. Shown for comparison are the gf values for the strongest 2p-3d transitions in  $\text{Mo}^{23+}$  and  $\text{Mo}^{24+}$ . These gf values were computed using the HXR method of calculating radial wavefunctions, including the Slater-Condon theory of atomic structure<sup>1,2</sup>. The bumps at 4.9 and 5.1 Å are in good agreement with the predicted 2p-3d lines of  $\text{Mo}^{23+}$  and  $\text{Mo}^{24+}$ , supportive of coronal equilibrium calculations<sup>3</sup> which predict the predominant molybdenum charge states at 900 eV to be near  $\text{Mo}^{23+}$  and  $\text{Mo}^{24+}$ .

Fig. 3 is the spectrum at 20 ms, during the spike of the SBD signal. Shown for comparison are the predicted gf values for the 2s-3p, 2p-3d, and 2p-3s transitions of  $\text{Mo}^{32+}$  and  $\text{Mo}^{31+}$  as well as the 2p-3d transitions for  $\text{Mo}^{30+}$ . Again, the wavelength agreement is quite good. The relative heights of the observed 2p-3s lines to the 2p-3d lines are considerably larger than the gf value ratio. This has been observed elsewhere<sup>4</sup> for  $\text{Mo}^{32+}$ . These charge state identifications are again in agreement with coronal equilibrium calculations<sup>3</sup> which predict the predominant charge states at 1800 eV to be  $\text{Mo}^{30+}$ ,  $\text{Mo}^{31+}$ , and  $\text{Mo}^{32+}$ . However, this

is neither a steady state nor thermal portion of the discharge and these particular coronal equilibrium calculations are not necessarily a priori valid.

There remains to explain the feature at  $4.44 \text{ \AA}$  (2.79 keV) in Fig. 2. Fig. 4 exhibits a more detailed scan of this feature for discharges similar to the one described above. Also shown are the predicted wavelengths for the K lines of<sup>5</sup> heliumlike  $\text{Cl}^{15+}$ . The agreement is quite good. Again, coronal equilibrium calculations<sup>3</sup> suggest that the predominant charge state for  $400 \text{ eV} \leq T_e \leq 1500 \text{ eV}$  is  $\text{Cl}^{15+}$ . This is consistent with the observation on Alcator A that this line prevails for a range of central electron temperature between 700 and 1200 eV. The molybdenum features between 4.6 and  $5.1 \text{ \AA}$  shift as the electron temperature is altered as expected from changes in charge states. These observations support both the wavelength predictions and the coronal equilibrium calculations.

Chlorine radiation has been seen in the UV and visible regions as well. In particular, the 2s-2p transition of  $\text{Cl}^{14+}$  at  $384 \text{ \AA}$  and the 3s-3p transitions of  $\text{Cl}^{6+}$  at 813 and  $801 \text{ \AA}$  have been observed with a spatial imaging detection system (SIDS)<sup>6</sup>. Fig. 5 is a spatial brightness profile of the  $384 \text{ \AA}$  line. The points outside  $\pm 5 \text{ cm}$  represent contamination from the bright  $\text{C}^{\text{IV}}$  line also at  $384 \text{ \AA}$  but located at a larger radial position. The  $4795 \text{ \AA}$  line of  $\text{Cl}^{\text{II}}$  has been observed during discharge cleaning. The  $384 \text{ \AA}$  line has been seen in TFR<sup>7</sup> discharges.

A possible source for the chlorine is the solvent trichloroethane used in cleaning Alcator vacuum components. Chlorine may also be a contaminant of the stainless steel vacuum bellows. The source of the molybdenum is the Mo limiter used in Alcator A. Further evidence that the  $4.44 \text{ \AA}$  feature is not due to molybdenum radiation has been provided by a series of impurity injection experiments. In one such case Mo was introduced into the plasma by the laser blowoff technique<sup>8</sup>, and Fig. 6a demonstrates the result. The top trace is the average electron density and the rise of the spike in the second trace indicates the time of the laser firing which injected the molybdenum. The third trace is the SBD flux ( $h\nu > 1.5 \text{ keV}$ ) which exhibits a bump similar to that shown in Fig. 1. The fourth trace is the spectrometer signal at  $5.20 \text{ \AA}$  ( $2.38 \text{ keV}$ ) showing a factor of 8 or so increase in signal after the injection. Fig. 6b is a blowup of Fig. 6a near the region of interest ( $2 \text{ ms/div}$ ). It seems to take about 6 - 10 ms for the molybdenum to reach the center of the discharge after the injection and the molybdenum remains in the plasma for about 15 ms. Fig. 7 shows a similar trace but with the spectrometer set on  $4.44 \text{ \AA}$ . The SBD trace demonstrates the induced Mo radiation at  $\sim 50 \text{ ms}$  as well as the naturally occurring bump at 25 ms. Neither of these features is present on the  $4.44 \text{ \AA}$  trace indicating that this line is not due to molybdenum.

On the bottom of Fig. 2, an X indicates an observed increase in signal at that wavelength when molybdenum is injected into the plasma and an 0 indicates no change.

From the strength of the Cl K line above the continuum background, one may deduce an estimate of the chlorine density in Alcator A. If one equates the ratio of the observed line to continuum to the ratio of the number of 1s vacancies in  ${}^9\text{Cl}^{15+}$  to the number of continuum photons<sup>10</sup> produced, one obtains (ignoring profile effects)

$$\frac{I_{\text{Cl}}}{I_{\text{cont}}} = \frac{1.6 \times 10^{-5} n_e n_{\text{Cl}} \langle g \rangle f_{\text{nn}^*} e^{-\Delta E/T_e}}{\Delta E \sqrt{T_e}} \cdot \frac{9.58 \times 10^{-14} n_e^2 \xi \bar{g} e^{-h\nu/T_e} \Delta h\nu}{h\nu \sqrt{T_e}} \quad (1)$$

where  $f_{\text{nn}^*}$  is the oscillator strength of the transition of energy  $\Delta E$ ,  $\langle g \rangle$  and  $\bar{g}$  are gaunt factors,  $\xi$  is the bremsstrahlung enhancement factor, and  $\Delta h\nu$  is the resolution of the instrument. Solving for  $n_{\text{Cl}}$  and taking  $I_{\text{Cl}}/I_{\text{cont}} = 9$ ,  $n_e = 3 \times 10^{14} \text{cm}^{-3}$ ,  $\xi = 1$ ,  $\langle g \rangle = .2$ ,  $f_{\text{nn}^*} = .8$ ,  $\bar{g} = .7$ ,  $T_e = 900 \text{ eV}$ ,  $\Delta h\nu = 40 \text{ eV}$ , and  $\Delta E = h\nu = 2.79 \text{ keV}$ , one obtains a chlorine density of  $3 \times 10^9 \text{cm}^{-3}$  or  $10^{-5} n_e$ .

From this amount of chlorine, an estimate may be made of its contribution to radiative power loss in the plasma. Taking the cooling rate of chlorine at 900 eV to be  $2.5 \times 10^{-27} \text{ watt/cm}^3$  (this is actually the value for sulphur<sup>11</sup>), and electron and chlorine densities to be  $3 \times 10^{14} \text{cm}^{-3}$  and  $3 \times 10^9 \text{cm}^{-3}$ , respectively, one obtains a radiated power density of  $.0023 \text{ watt/cm}^3$  from the center of the plasma. This is a mere .015% of the central input ohmic power density for the

typical case of  $15 \text{ watt/cm}^3$ , and chlorine does not enter in a significant way to power balance in Alcator A.

### III. Conclusions

Observations of Mo L lines from  $\text{Mo}^{22+} \leq \text{Mo}^{i+} \leq \text{Mo}^{32+}$  and Cl K lines from  $\text{Cl}^{15+}$  have been made on the Alcator A tokamak, supportive both of wavelength predictions and coronal equilibrium calculations. Estimates indicate that  $n_{\text{Cl}}/n_e$  is of order  $10^{-5}$ , therefore not important in power balance considerations.

### IV. Acknowledgements

Thanks are due Herb Schnopper for providing the instrument used in these measurements, Dave Stallard for technical support, and Dave Overskei for operating Alcator A.

## References

1. R.D. Cowan and D.C. Griffin, J. Opt. Soc. Am. 66, 1010 (1976).
2. R.D. Cowan, J. Opt. Soc. Am. 58, 808, 924 (1968).
3. C. Breton, C. DeMichelis, M. Finkenthal, and M. Mattioli, EUR - CEA - FC - 948 (1978).
4. P. Burkhalter, R. Schneider, C.M. Dozier and R.D. Cowan, Phys. Rev. A 18, 718 (1978).
5. R.L. Kelly and L.J. Palumbo, NRL Report 7599 (1973).
6. R.K. Richards, H.W. Moos, and S.L. Allen, Rev. Sci. Instr. 51, 1 (1980).
7. Equipe TFR CUR - CEA - FC - 984 (1979).
8. E.S. Marmar, J.L. Cecchi and S.A. Cohen, Rev. Sci. Instr. 46, 1149 (1975).
9. R.C. Elton, Methods of Experimental Physics, Vol. 9, Part A, p. 115, Academic Press, 1970.
10. J. Greene, Ap. J. 130, 693 (1959)



11. D.E. Post, R.V. Jensen, C.B. Tartar, W.H. Grasberger  
and W.A. Locke, Atomic Data and Nucl. Tables 20, No. 5,  
397 (1977).

## Figure Captions

Fig. 1. Typical 60 kG Alcator A discharge. Top trace 50 kA/div, second trace  $1 \times 10^{14} \text{ cm}^{-3}$ /fringe, time scale 20 ms/div.

Fig. 2. Brightness vs. wavelength at 100 ms for discharges similar to Fig. 1. Predicted gf values for 2p-3d transitions in  $\text{Mo}^{23+}$  and  $\text{Mo}^{24+}$ .

Fig. 3. Spectrum at 20 ms. Predicted gf values for  $\text{Mo}^{30+}$ ,  $\text{Mo}^{31+}$ , and  $\text{Mo}^{32+}$  L lines.

Fig. 4. More detailed scan of  $\text{Cl}^{15+}$  K lines near  $4.44 \text{ \AA}$ .

Fig. 5. Radial brightness profile at  $384 \text{ \AA}$ .

Fig. 6a. Molybdenum injection, 20 ms/div. 6b. Expanded view of injection, 2 ms/div.

Fig. 7. Molybdenum injection showing no effect at  $4.44 \text{ \AA}$ .

Typical Alcator A Discharge at 60 KG

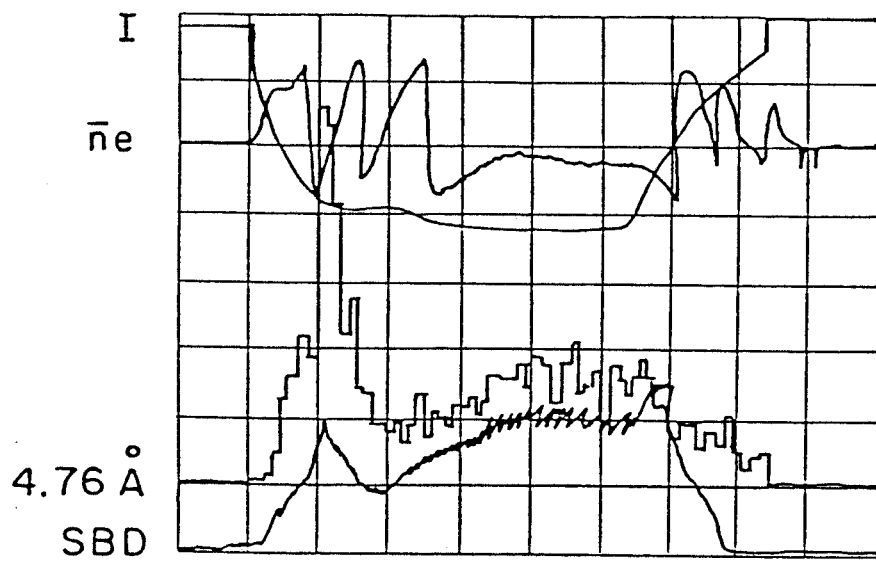
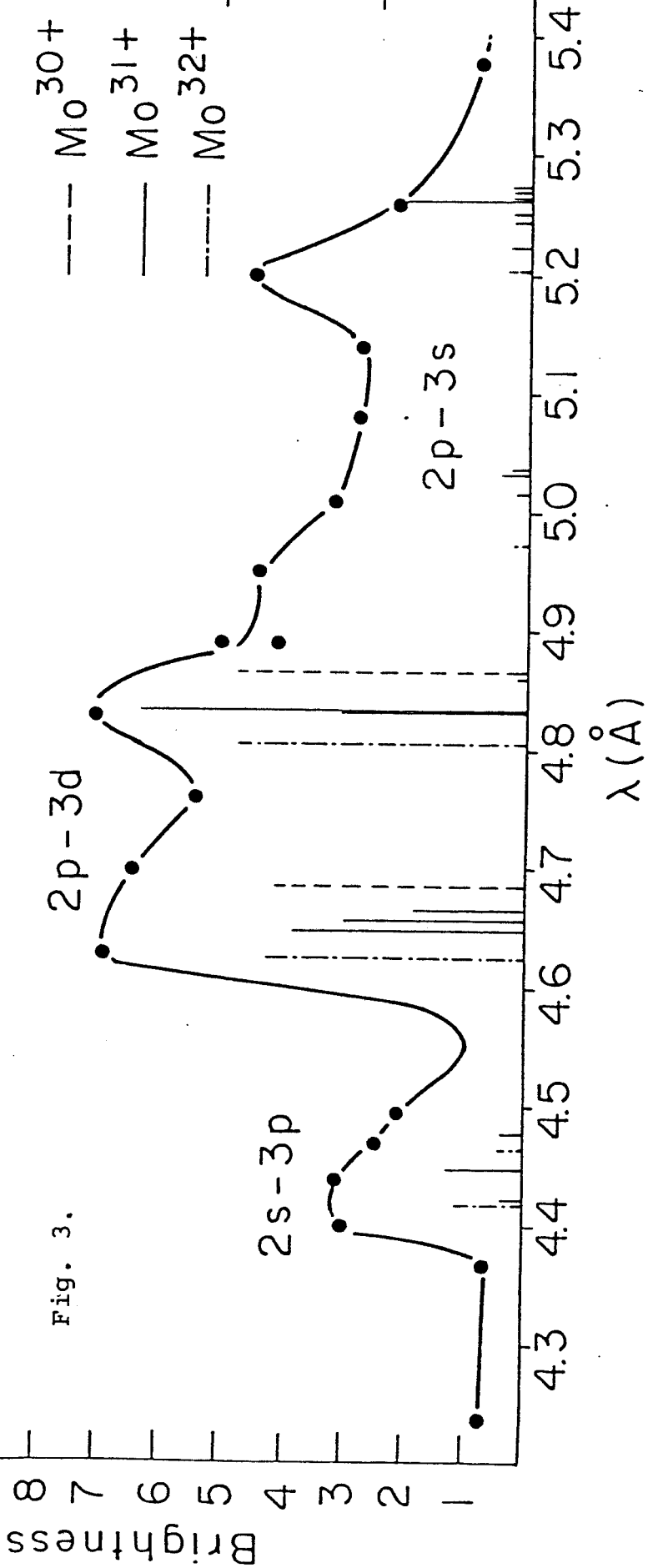
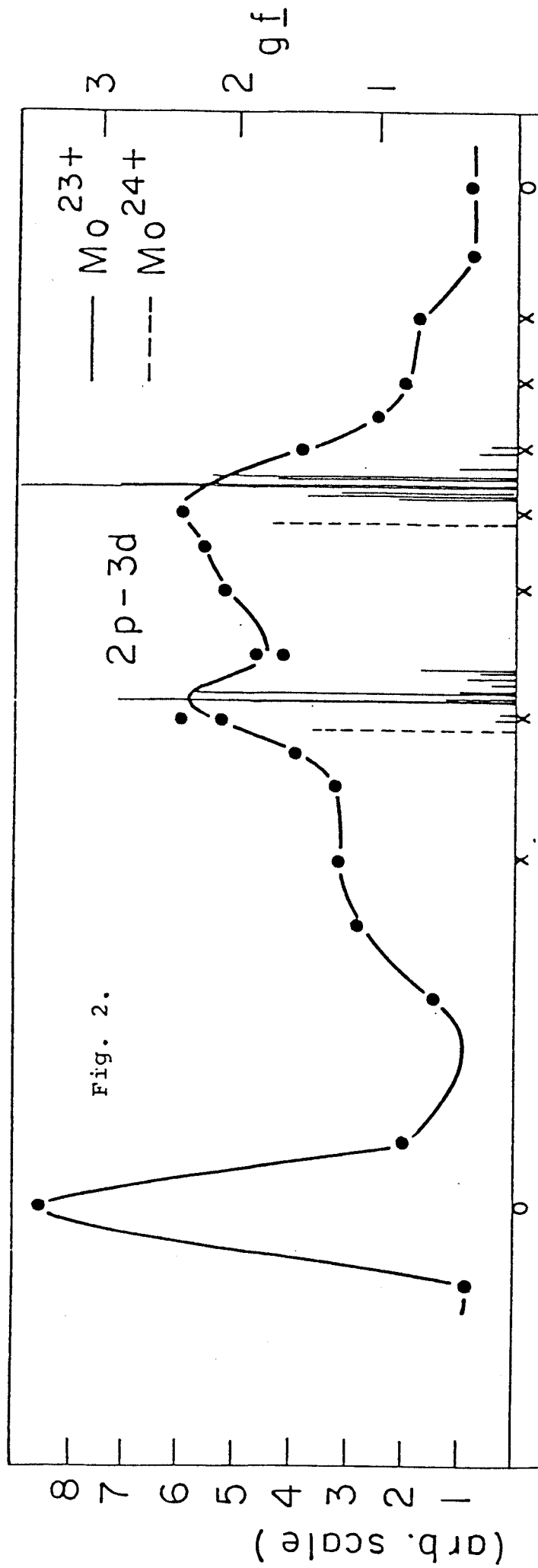


Fig. 1.



CI <sup>15+</sup>

1s<sup>2</sup>-1s2p

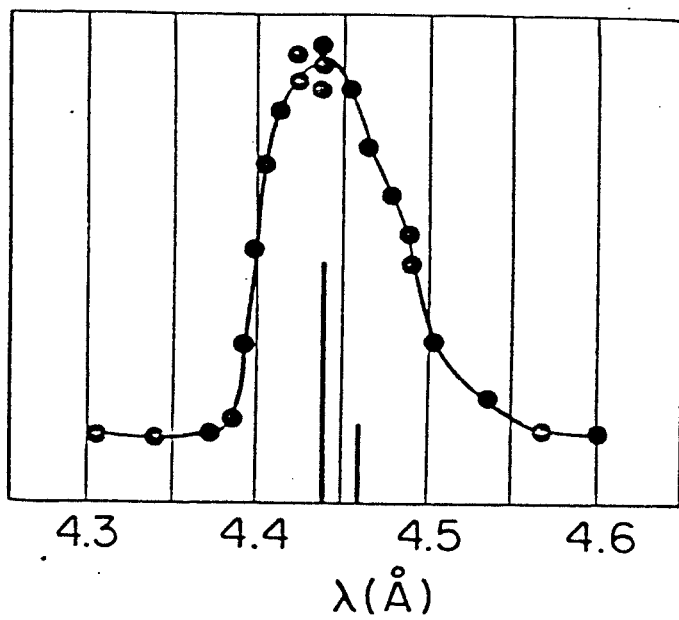


Fig. 4.

384Å Cl<sup>14+</sup>  
Brightness Profile

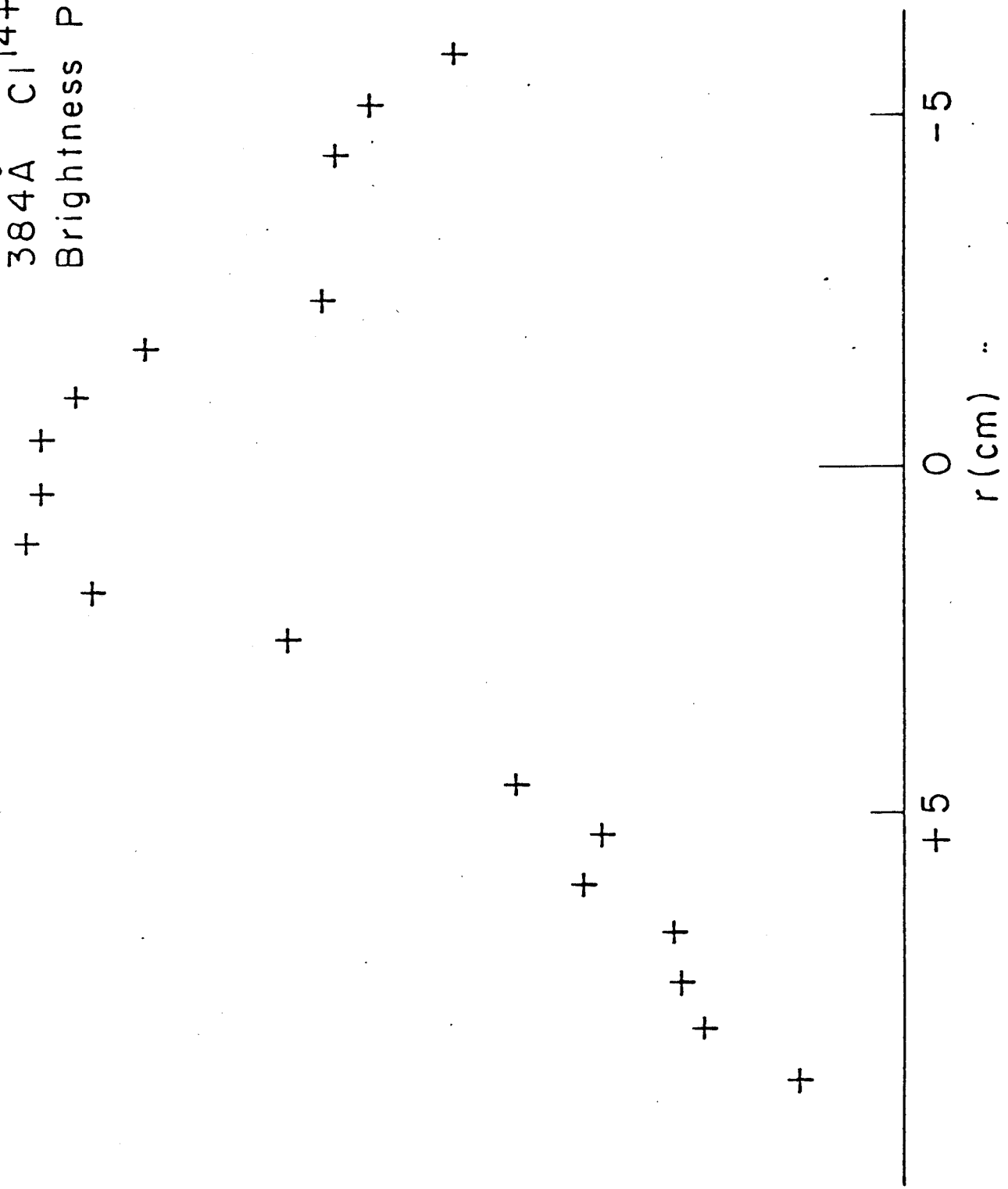
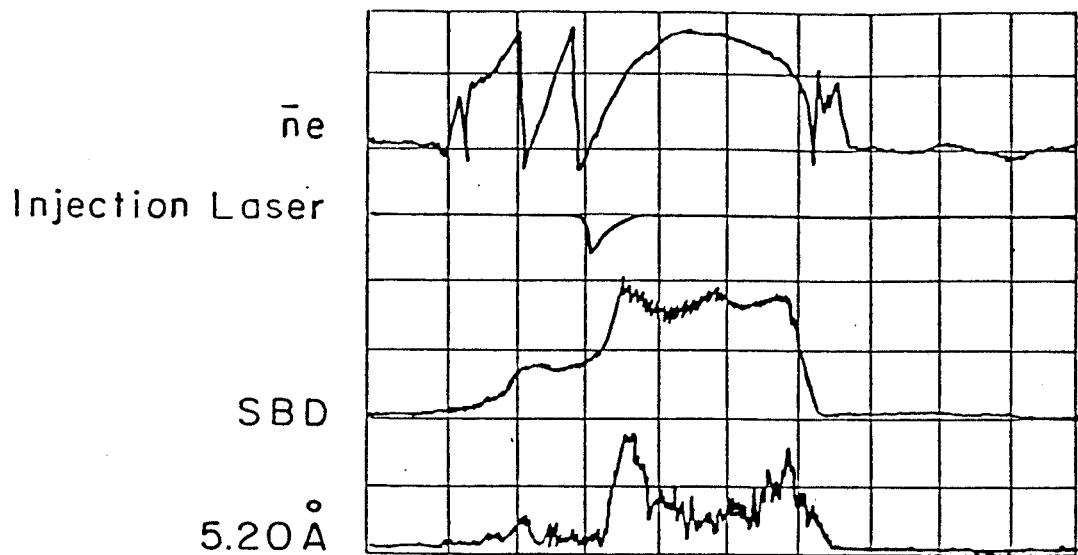


Fig. 5.

# Molybdenum Injection (a)



(b)

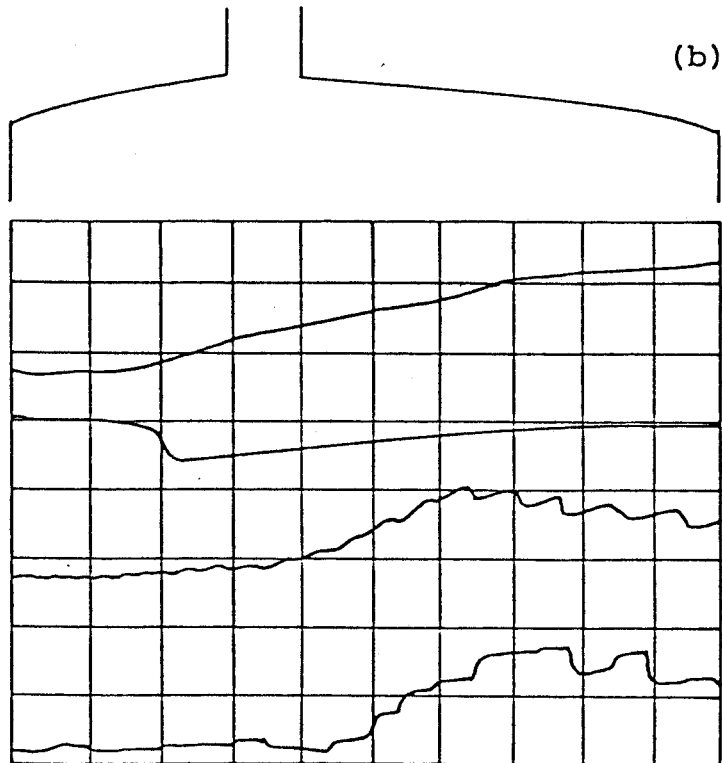


Fig. 6.

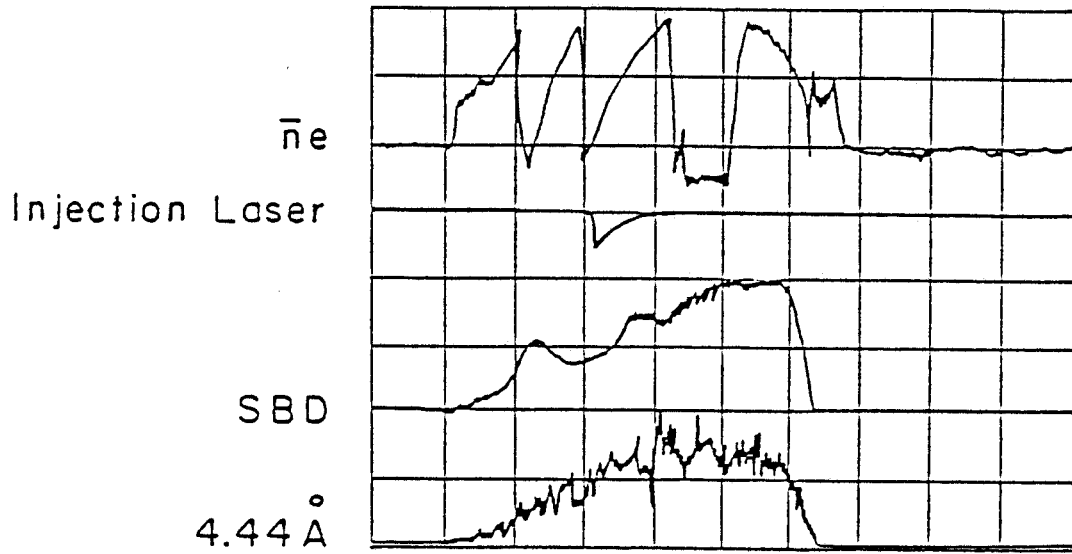


Fig. 7.